Electronic supplementary materials *Mendeleev Commun.*, 2023, **33**, 267–268

Ferromagnetism in fast temperature quenched cobalt-doped chalcopyrites $Cu_{1-x/2}In_{1-x/2}Co_xSe_2$

Mikhail A. Zykin, Svetlana V. Golodukhina and Nikolay N. Efimov

1. Synthesis

All samples **1-5** were synthesized by two-stage stair-step procedure depicted on Fig. S1 (first stage is shown in black and second in red).

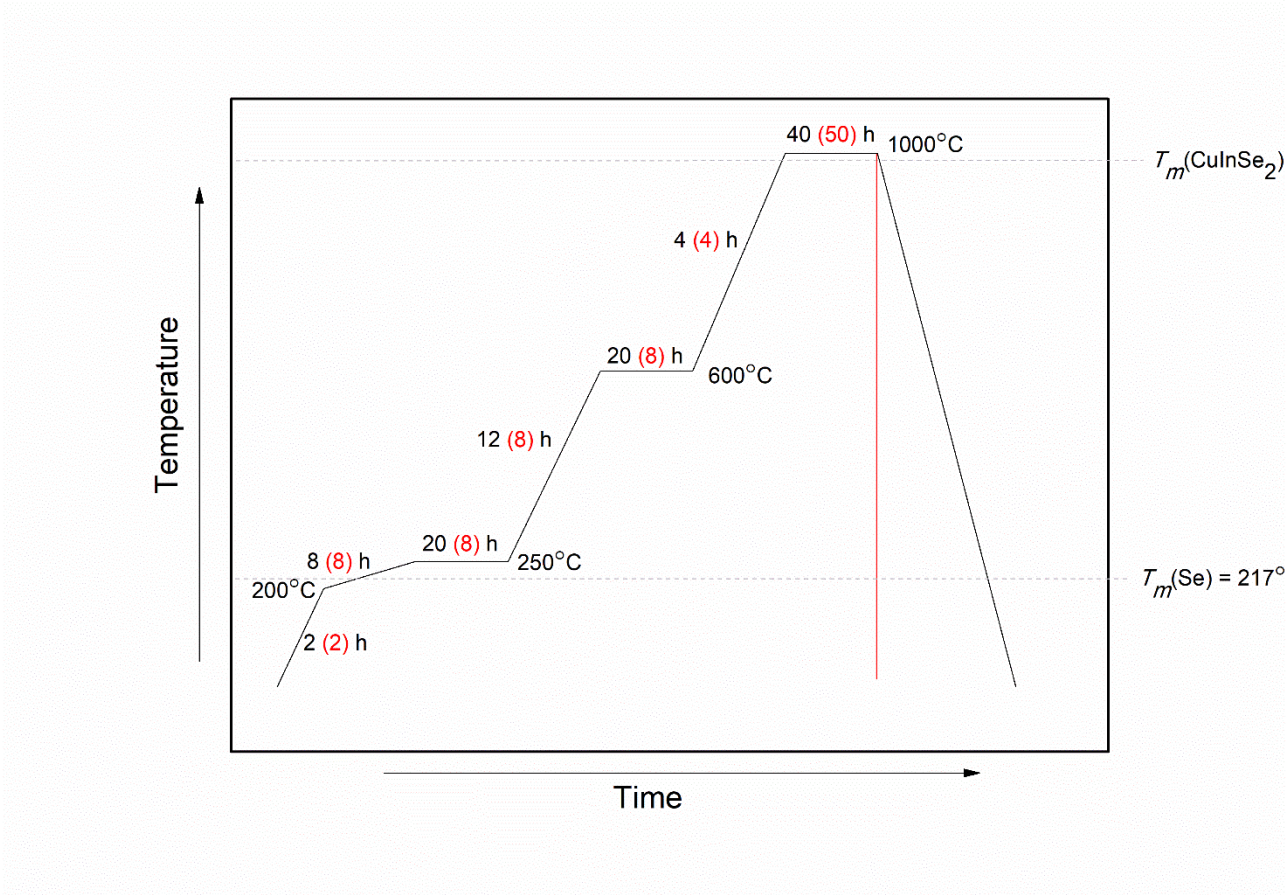

Figure S1 Scheme of the synthesis of the samples. Temperature and duration of each step are shown (not to scale). Preliminary stage (that was finished by slow cooling) is shown by black and final stage with water quenching is shown by red. Melting points of selenium (initial compound) and $CuInSe_2$ chalcopyrite are also shown.

To start the first stage, elemental compounds of Cu (chemical grade, powder), In (Sigma Aldrich, 99.95%, bars), Se (Sigma Aldrich, 99.5%, powder) and Co (chemical grade, chips) were mixed together in evacuated (residual pressure not worse than 0.03 Pa) quartz ampoules in stoichiometric ratio, sealed and putted in vertical tubular furnace. Then stair-step regime (Fig. S1, black numbers) was realized. This regime includes slow heating through melting point of selenium to avoid sharp increasing of pressure and ampoules' crushing and final heating slightly above of target $CuInSe_2$ melting point. First stage finished by slow cooling of ampoules in furnace. After that ampoules were crushed, black polycrystalline powders were extracted, reground in agate mortar and searched by powder X-rays diffraction (**XRD**) phase analysis and magnetic measurements. The samples of cobalt-doped $CuInSe_2$ were obtained as a result of the first stage.[1]

The second stage (Fig. S1, red numbers) is nearly the same as the first but with a little shorter times (the samples contain much lower, if any, quantity of elemental selenium). Powders of chalcopyrites were again putted into evacuated quartz ampoules (residual pressure not worse than 0.003 Pa), sealed and annealed. The stage was finished by rapid quenching of ampoules from hot (1000°C) furnace to room-temperature water. Then ampoules were crushed, samples were ground and searched by XRD, magnetometry and electron microscopy.

2. Physical analytical methods

XRD analysis was performed on Bruker D8 Advance diffractometer (Cu Kα radiation, Bragg-Brentano geometry).

Magnetometry was made with PPMS-9 Quantum Design magnetometer. Powder samples were mixed with diamagnetic oil, sealed in polyethylene bag and placed in plastic straw to put inside the magnetometer. The measured magnetic data were corrected on diamagnetism of oil, polyethylene bag, plastic straw and intrinsic core diamagnetism of the samples (Pascal's corrections[2]). Isothermal magnetization *vs.* magnetic field $M(H)$ dependencies were measured at different temperatures T = 2, 35 and 300 K in the magnetic field range of ±50 kOe. Magnetization *vs.* temperature $M(T)$ measurements were performed at magnetic field H = 5 kOe in the temperature range 2-300 K. These data then were mathematically recalculated (for example from $M(T)$ in $\chi T(T)$ or $\chi^{-1}(T)$ form, where $\chi = M/H$ is magnetic susceptibility).

Electron microscopy was performed using a high resolution scanning electron microscope Carl Zeiss NVision 40 with the option of local X-ray spectral microanalysis, **EDX**.

3. XRD

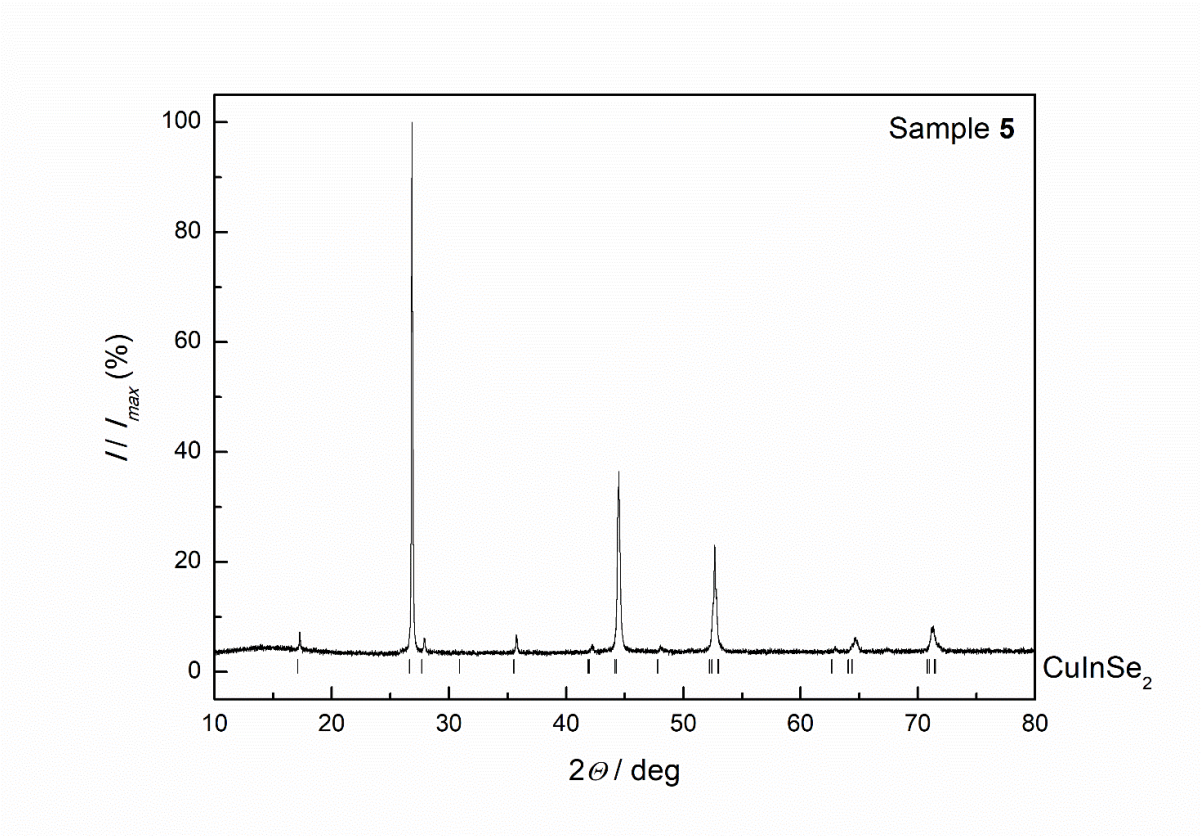

Figure S2 XRD pattern of the most concentrated synthesized sample **5** compared with reference ICSD card #80-2189 ($CuInSe_2$) that is shown by strokes at the bottom.

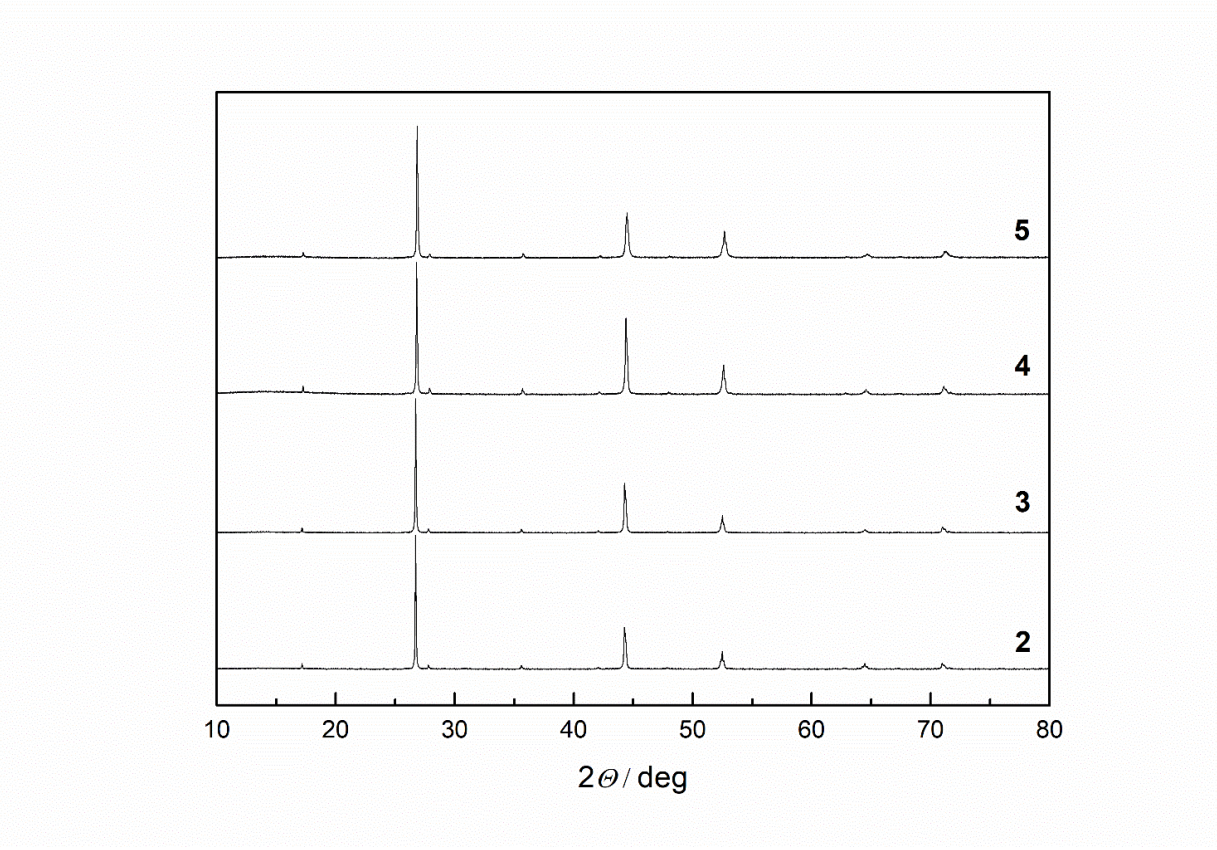

Figure S3 XRD patterns of all synthesized samples.

Table S1. Unit cell parameters *a*, *c* and volume *V* of synthesized quenched samples compared with parent unquenched samples.[1]

Sample	without quenching[1]			quenched (this work)		
	a, Å	*c*, Å	*V*, Å^3	*a*, Å	*c*, Å	*V*, Å^3
1	5.7842(6)	11.6210(18)	388.8(1)			
2	5.7800(4)	11.6139(9)	388.00(6)	5.7823(9)	11.5962(22)	387.72(15)
3	5.7787(3)	11.6132(6)	387.80(4)	5.7791(9)	11.5849(20)	386.91(14)
4	5.7749(16)	11.600(2)	386.84(21)	5.7762(10)	11.5800(22)	386.36(17)
5	5.7657(16)	11.567(3)	384.5(3)	5.7679(14)	11.582(3)	385.33(23)

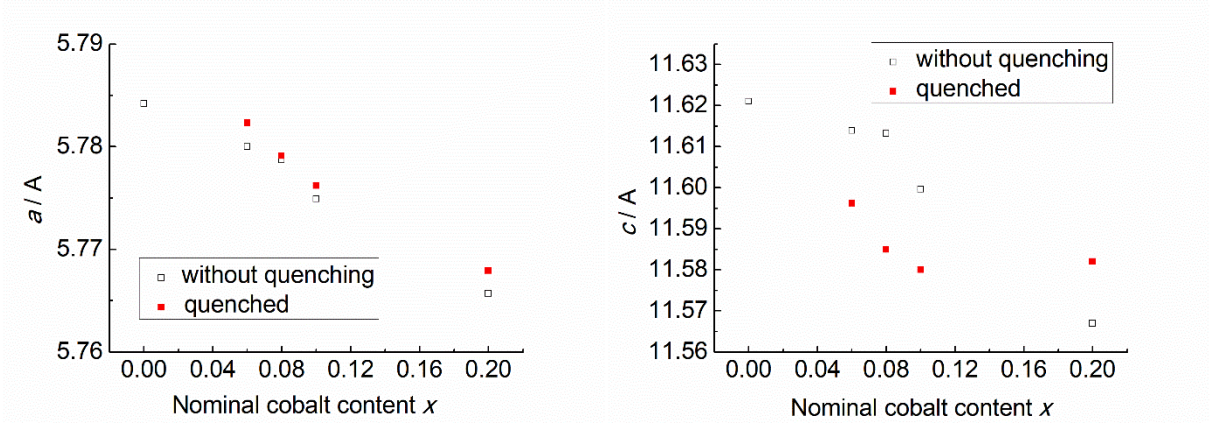

Figure S4 Unit cell parameters *a* (left) and *c* (right) *vs.* nominal cobalt content plots for all synthesized samples (shown by red filled squares) compared with parent unquenched samples[1] (shown by open black squares).

4. Magnetic properties: *M*(*H*)

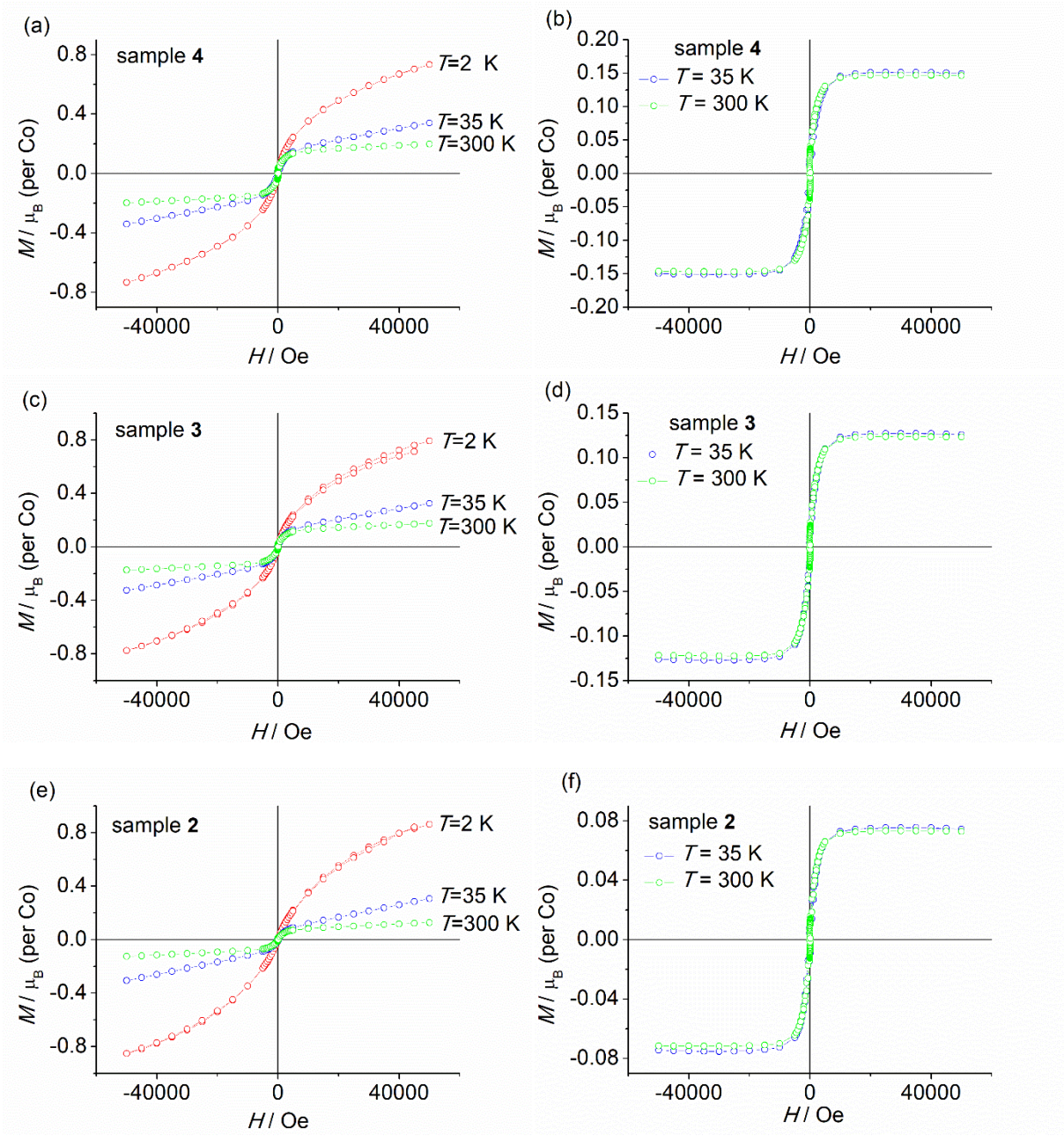

Figure S5 Isothermal magnetization curves measured at temperatures T = 2, 35 and 300 K (left: a), c), e)) and "ferromagnetic" isothermal magnetization curves for temperatures T = 35 and 300 K obtained by subtraction of linear part from measured curves (see main text for details) (right: b), d), f)) for the samples **4** (a), b)), **3** (c), d)) and **2** (e), f)). The same data for the sample **5** are given in the main text. All data are calculated per cobalt content.

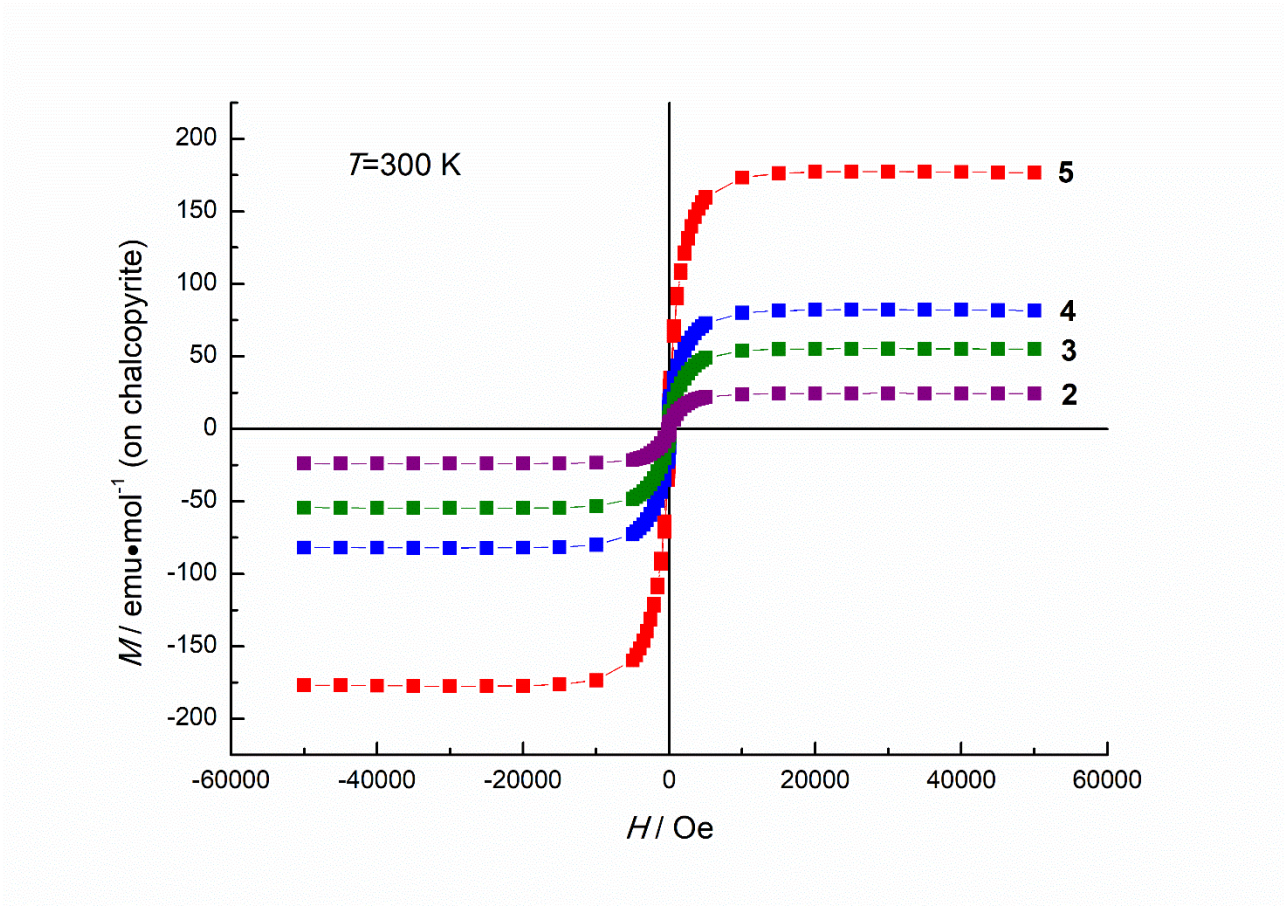

Figure S6 Isothermal "ferromagnetic" molar magnetization (calculated per chalcopyrite content) *vs.* magnetic field curves after subtracting linear part at temperature T = 300 K for all synthesized samples.

Table S2. Magnetic characteristics extracted from hysteresis loops $M(H)$ for all synthesized samples at different temperatures T = 2, 35 and 300 K: remanent magnetization M_r, saturation magnetization M_S (in Bohr magneton per cobalt, μ_B), M_r/M_S ratio, and coercive field H_C.

T	2 K	35 K				300 K			
Sample	M_r, μ_B	M_r, μ_B	M_s, μ_B	M_r/M_s	H_c, Oe	M_r, μ_B	M_s, μ_B	M_r/M_s	H_c, Oe
2	0.0090	0.0099	0.075	0.13	263	0.0091	0.072	0.13	134
3	0.0140	0.0150	0.127	0.12	207	0.0163	0.122	0.13	128
4	0.0237	0.0237	0.151	0.16	295	0.0283	0.147	0.19	140
5	0.0166	0.0155	0.163	0.095	140	0.0147	0.159	0.09	83

5. Magnetic properties: *M*(*T*)

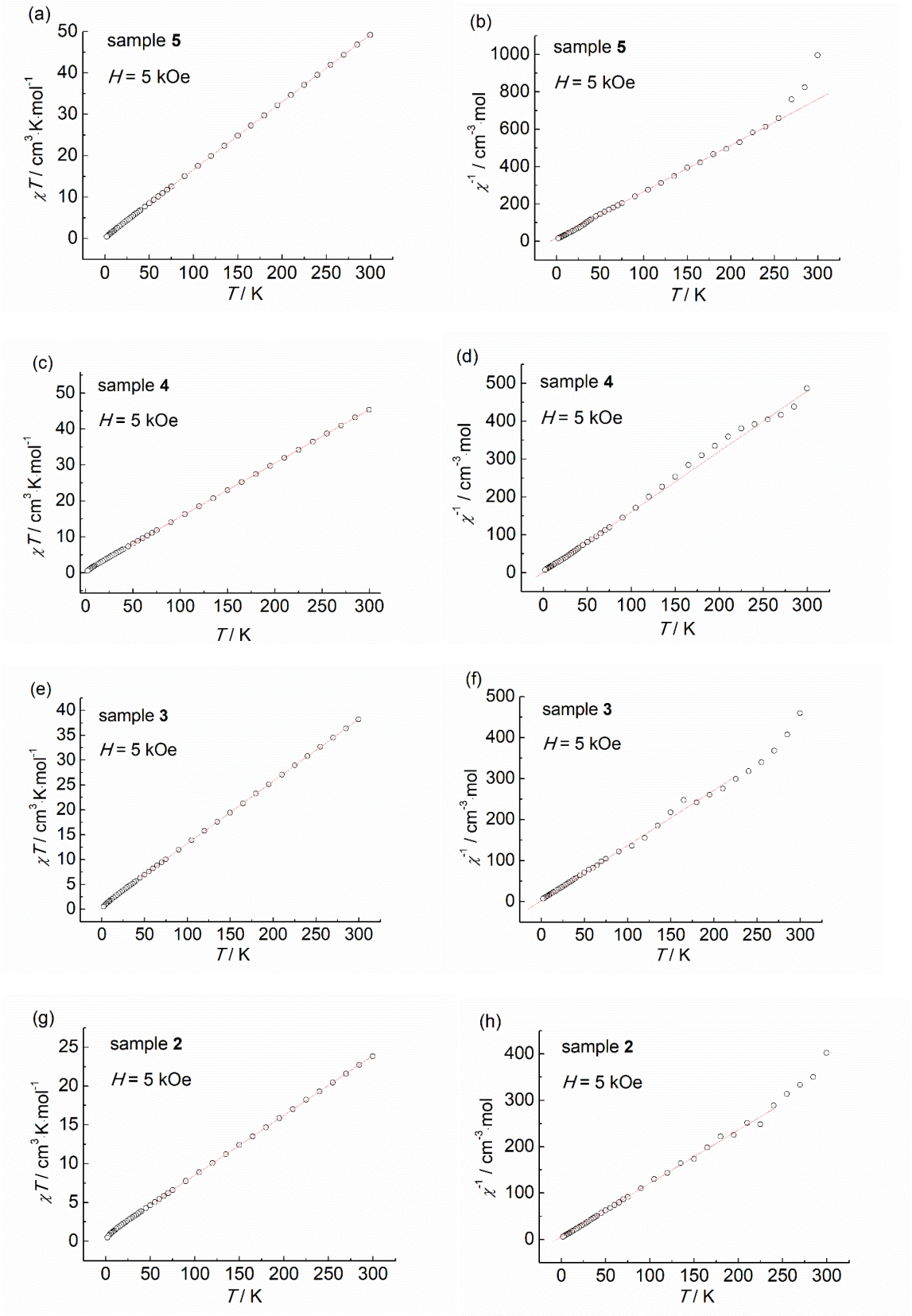

Figure S7 χT *vs. T* dependencies (left: a), c), e), g)) and χ^{-1} *vs. T* dependencies (right: b), d), f), h)) for all synthesized samples. All data calculated per cobalt content.

Table S3. Magnetic data for all synthesized samples extracted from $M(H)$ dependencies (column **A**, Fig. 2 and S5) and $M(T)$ dependencies (column **B**, Fig. S7aceg). M_S – saturation magnetization, M_{5000} – magnetization at magnetic field H = 5000 Oe, χ_{FIP} – magnetic field-independent magnetic susceptibility (extracted from linear part of $M(H)$ dependencies). χ_{TIP} – temperature-independent magnetic susceptibility (extracted from linear part of χT *vs.* T dependencies), M_{TIP} – temperature-independent magnetization derived from χ_{TIP} just multiplying by 5000 (because χT *vs.* T dependencies were measured at magnetic field H = 5000 Oe, given to compare with M_{5000}), χ_{const} = (M_{TIP}-M_{5000})/5000 – temperature-and-field-independent magnetic susceptibility, χ_{para} – temperature-dependent magnetic susceptibility (obtained by subtracting χ_{TIP} from $\chi(T)$).

Sample	T, K	**A**			**B**			
		M_S, emu/mol	M_{5000}, emu/mol	χ_{FIP}, cm^3/mol	χ_{TIP}, cm^3/mol	M_{TIP}, emu/mol	χ_{const}, cm^3/mol	χ_{para}, cm^3/mol
5	300	885	797	0.00465(7)	0.16304(6)	815	0.0036	0.00101
	35	910	795	0.01315(11)			0.0040	0.0097
4	300	821	728	0.00574(7)	0.14944(6)	747	0.0038	0.00206
	35	845	707	0.02131(14)			0.0080	0.0176
3	300	687	607	0.00583(5)	0.12519(8)	626	0.0038	0.00218
	35	710	613	0.02221(9)			0.0026	0.0199
2	300	404	365	0.00612(3)	0.07702(13)	385	0.0040	0.00249
	35	421	368	0.02590(8)			0.0034	0.0224

Table S4. Magnetic data for all synthesized samples obtained by fitting of $\chi^{-1}(T)$ dependencies (Fig. S7bdfh) by linear function (Curie-Weiss law): $\chi^{-1} = (T+\Theta)/C$. C – Curie constant, Θ – Weiss constant, x_P – mole fraction (per chalcopyrite) of paramagnetic cobalt that obtained from nominal cobalt content x as follow: $x_P = C*x/2.27$, where 2.27 is theoretical value of C for Co^{2+} (spin S = 3/2, g-value g = 2.2), x_{Pwq} – analogous x_P for the parent unquenched samples (from Ref. 1).

Sample	C, cm^3·K/mol	Θ, K	x_P	x_{Pwq}[1]
5	0.405(2)	8	0.036	0.026
4	0.628(8)	0.6	0.028	0.022
3	0.750(19)	3.1	0.026	0.021
2	0.870(17)	5.2	0.023	0.018

6. Electron microscopy

Table S5. Chemical composition of **4** by EDX data.

Sample **4**	Atomic fraction				Atomic content normalized on Cu			
	Co	Cu	Se	In	Co	Cu	Se	In
nominal value					0.1	0.95	2	0.95
point 1	2.60	23.70	48.27	25.43	0.1042	0.95	1.9349	1.0193
point 2	2.56	24.45	47.36	25.63	0.0995	0.95	1.8402	0.9958
point 3	2.15	18.82	56.22	22.80	0.1085	0.95	2.8379	1.1509
point 4	2.51	22.38	50.61	24.49	0.1065	0.95	2.1483	1.0396
point 5	2.04	19.95	54.82	23.19	0.0971	0.95	2.6105	1.1043
point 6	2.25	21.14	53.89	22.72	0.1011	0.95	2.4217	1.0210
average					**0.103(4)**	**0.95**	**2.3(4)**	**1.06(6)**

Figure S8 Electron microscope image of **4**.

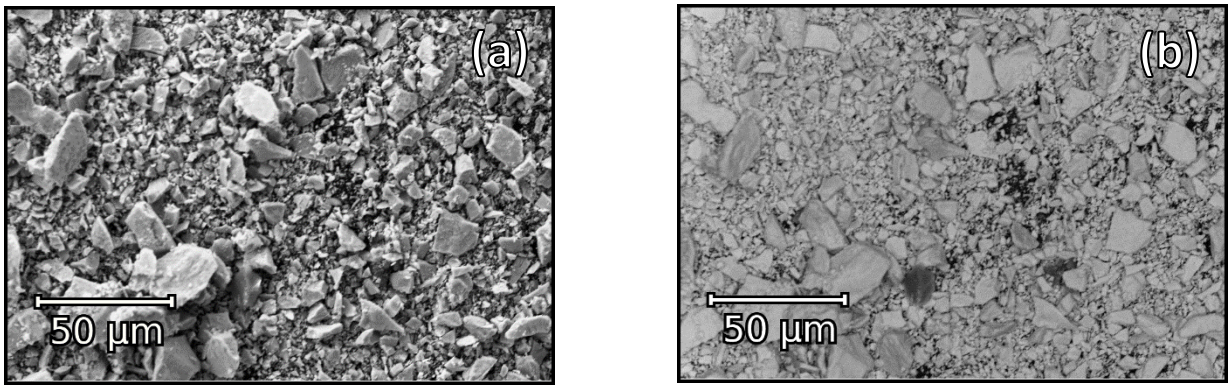

Figure S9 Electron microscope image of **4**: topography obtained with SE2 detector (a) and composition contrast obtained with ESB detector (b). The more darker particles in image b are pieces of quartz SiO_2 (confirmed by EDX).

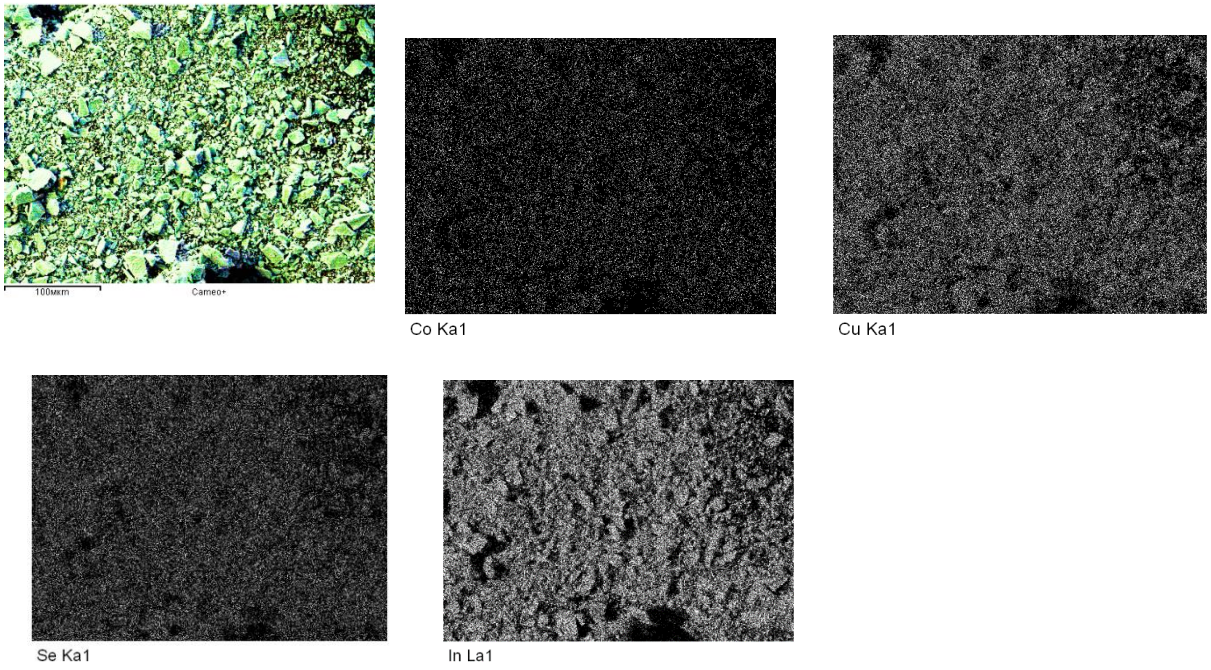

Figure S10 A cameo+ image and the results of EDX mapping elements from one of the studied areas of **4**.

7. References

S1. M. A. Zykin and N. N. Efimov, *Russ. Chem. Bull.*, 2022, **71**, 701.

S2. G. A. Bain and J. F. Berry, *J. Chem. Educ.*, 2008, **85**, 532.